Two pairs of topological Shockley surface bands in the ternary compound $SnSb_2Te_4$

H. J. Qian,[1,2] J. M. Wang,[1,2] D. Y. Wang,[1,2] Q. Jiang,[1,2] H. M. Zha,[1,2] W. J. Liu,[1,2] X. P. Shen,[3] M. Ye,[1,2,*] and S. Qiao[1,2,4,†]

[1]*Center for Excellence in Superconducting Electronics, State Key Laboratory of Functional Materials for Informatics, Shanghai Institute of Microsystem and Information Technology, Chinese Academy of Science, Shanghai 200050, People's Republic of China*

[2]*Center of Materials Science and Optoelectronics Engineering, University of Chinese Academy of Sciences, Beijing 100049, People's Republic of China*

[3]*State Key Laboratory of Surface Physics, Department of Physics, Fudan University, Shanghai 200433, People's Republic of China*

[4]*School of Physical Science and Technology, ShanghaiTech University, Shanghai 201210, People's Republic of China*

(Received 14 March 2022; accepted 6 June 2022; published 15 July 2022)

The electronic states in ternary compound $SnSb_2Te_4$ wwere studied by first-principles and tight-binding calculations, and two pairs of topological Shockley surface bands below its Fermi energy were revealed theoretically. One shows the Rashba-type structure and the other shows a more complicated ω-shaped bending structure. Combined with spin- and angle-resolved photoemission spectroscopy measurements, the existence of the predicted topological surface states was confirmed. Our theoretical and experimental investigations reveal the complex topological structures in ternary topological insulators, providing a new platform for studying novel topological properties in materials.

DOI: 10.1103/PhysRevB.106.045119

I. INTRODUCTION

Since the discovery of the 3D topological insulators (TIs), the spin-polarized Dirac surface states existing in their bulk band gaps have inspired enormous interest [1–12]. These special topologically protected surface states are caused by the inversion of topologically nonequivalent bulk bands. In the prototype TIs, such as the Bi_2Se_3 family and derived ternary ones, people have focused on the band inversions induced by the participation of spin-orbit coupling (SOC) and the topological Dirac surface states existing in the band gap between the conduction and the valence bands [3,7,10–12]. However, recent studies have shown that even in the absence of SOC, the bulk band inversions may still occur due to the crystal field in several materials, and special surface states known as Shockley states will lie in the inverted band gaps [13,14]. After including SOC, the band crossings will be gapped and topological Shockley surface states arise. In previous angle-resolved photoemission spectroscopy (ARPES) studies of the Bi_2Se_3 family, the Dirac topological surface states near the Fermi energy were thoroughly investigated. Although the existence of Rashba-type surface states below the Fermi energy was reported [15,16], their origin and topological properties were not studied. Besides, whether such Rashba-type surface states exist in the ternary ones of the Bi_2Se_3 family has not yet been investigated. Here we report the discovery of two different types of topological Shockley surface states in $SnSb_2Te_4$.

In previous studies [17], $SnSb_2Te_4$ was predicted to be a TI with a Dirac cone in the gap between valence and conduction bulk bands. Our calculated bulk band structure was consistent with previous ones. However, we will focus on the newly found topological Shockley surface states rather than the widely researched Dirac cone in this paper. Using tight-binding calculations, two pairs of Shockley surface bands were predicted, and the origin of their bulk band inversions was discussed with the results of density functional theory (DFT) calculations, revealing the nontrivial topological essence of the predicted Shockley surface states. One of these surface bands exhibited complicated ω-shaped bending, which is related to the inversions between three bulk bands. Combining with high-resolution ARPES (HRARPES) and spin-resolved ARPES (SARPES) measurements, the existence of the topological Shockley surface states below the Fermi energy was confirmed. Our results show the unique advantage and irreplaceability of SARPES to distinguish spin-split bands with tiny splitting. Furthermore, our study reveals the complex band structure of Shockley surface states in ternary TIs and provides a new avenue for studying the novel topological properties in materials.

II. EXPERIMENTS AND METHODS

Electronic band-structure calculations were performed in the framework of DFT using the Vienna ab initio simulation

*yemao@mail.sim.ac.cn.
†qiaoshan@mail.sim.ac.cn.

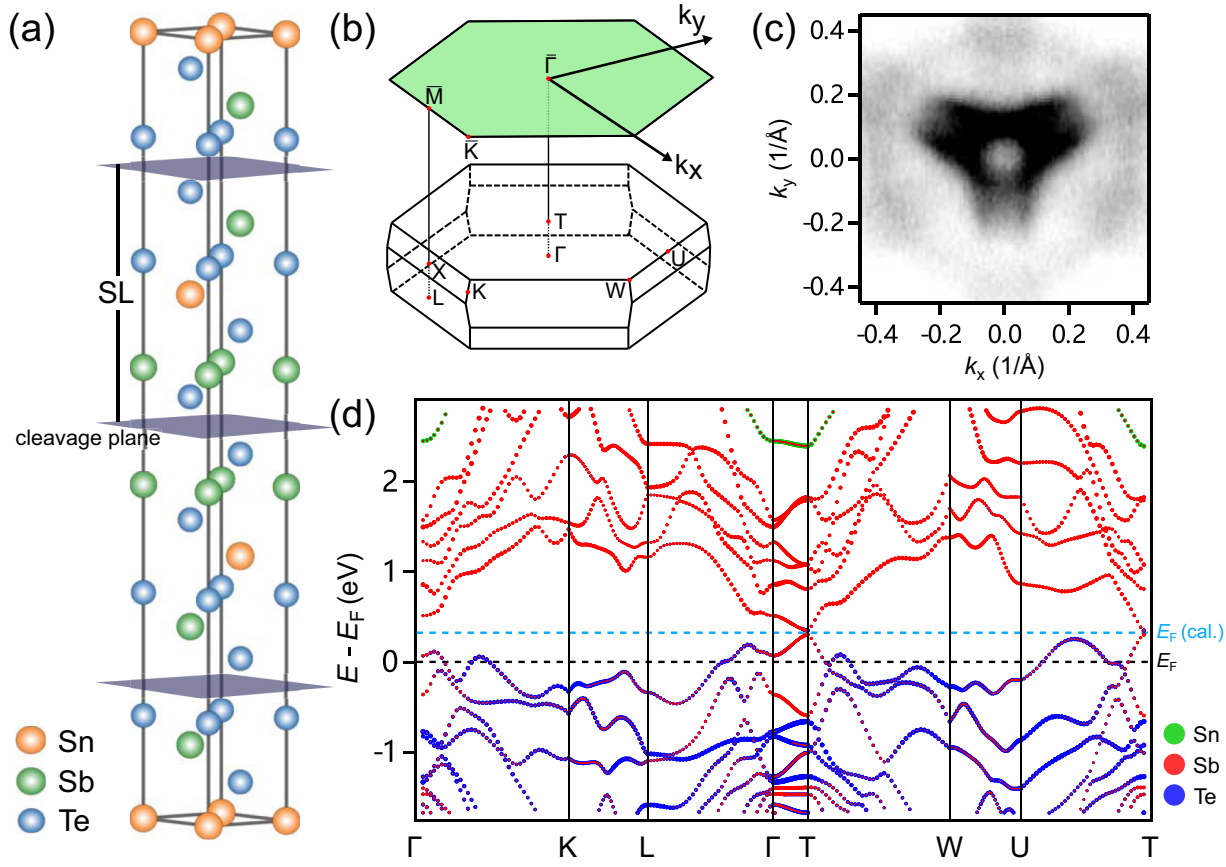

FIG. 1. Crystal structure and electronic band structure of $SnSb_2Te_4$. (a) The unit cell composed of three SLs with orange, green, and blue balls represent Sn, Sb, and Te atoms, respectively. (b) The first BZ of the bulk and the surface BZ projected onto the (111) surface (green plane). (c) Observed Fermi surface by HRARPES with 21 eV photon energy. (d) Calculated bulk band structure along high-symmetry directions in which the colors show the weight of the states at Sn (green), Sb (red), and Te (blue) atoms, respectively, with the blue dashed line indicating the location of calculated Fermi energy.

package with the Perdew-Burke-Ernzerhof method [18–20]. Surface electronic states were calculated by constructing localized Wannier functions [21,22] with the WANNIER-TOOLS package [23]. A single crystal of $SnSb_2Te_4$ was grown by using a self-flux method. First, a stoichiometric amount of Sn (99.99%, Alfa), Sb (99.99%, Alfa), and Te (99.99%, Alfa) powder was mixed and ground. Then, the mixture was sealed in a quartz ampule under a vacuum of 10^{-4} Pa. Subsequently, the ampule was heated to 1163 K and maintained for 4 h and then gradually cooled down to 773 K at a rate of 1 K/h and kept at 773 K for 150 h and then cooled down to room temperature with the furnace. The crystal is silvery shiny and easily cleavable. HRARPES measurements were performed at the BL03U beamline of the Shanghai Synchrotron Radiation Facility (SSRF) with a hemispherical electron-energy analyzer (Scienta-Omicron DA30) [24,25] at 15 K, with energy resolution ~10 meV, and 21 eV photons. SARPES measurements were performed on a home-made high-efficiency image-type SARPES spectrometer [26] at 7 K, with energy resolution ~12 meV, angular resolution ~0.25°, and 21.2 eV light from a He discharge lamp. The samples were cleaved *in situ* along the (111) plane with an ultrahigh vacuum of 10^{-8} Pa.

III. RESULTS

$SnSb_2Te_4$ has a rhombohedral primitive cell with a space group of $R\bar{3}m$ (No. 166). As shown in Fig. 1(a), its unit cell is composed of three septuple layers (SLs). The natural cleavage plane is between the adjacent Te layers of the two SLs. The bulk Brillouin zone (BZ) and the projected (111) surface BZ are shown in Fig. 1(b), with several high-symmetry points being indicated. The DFT calculated electronic band structure of bulk states is shown in Fig. 1(d), and the band compositions of Sn, Sb, and Te are denoted by green-, red-, and blue-filled circles, respectively. It is worth mentioning that the calculated Fermi energy is located at around 0.37 eV above the experimental one, as indicated by the dashed blue (calculated) and black (measured) lines.

According to the calculated bulk band structure shown in Fig. 1(d), Te p orbitals are dominant near the Fermi energy. The effect of SOC to the band structure is shown in Fig. 2(a) and the black (red) curves represent bands with (without) SOC. The calculations show that there are crystal-field-induced band inversions along the T-W direction even in the absence of SOC, and three band inversion-induced crossing points in the blue rectangle region are clearly observed,

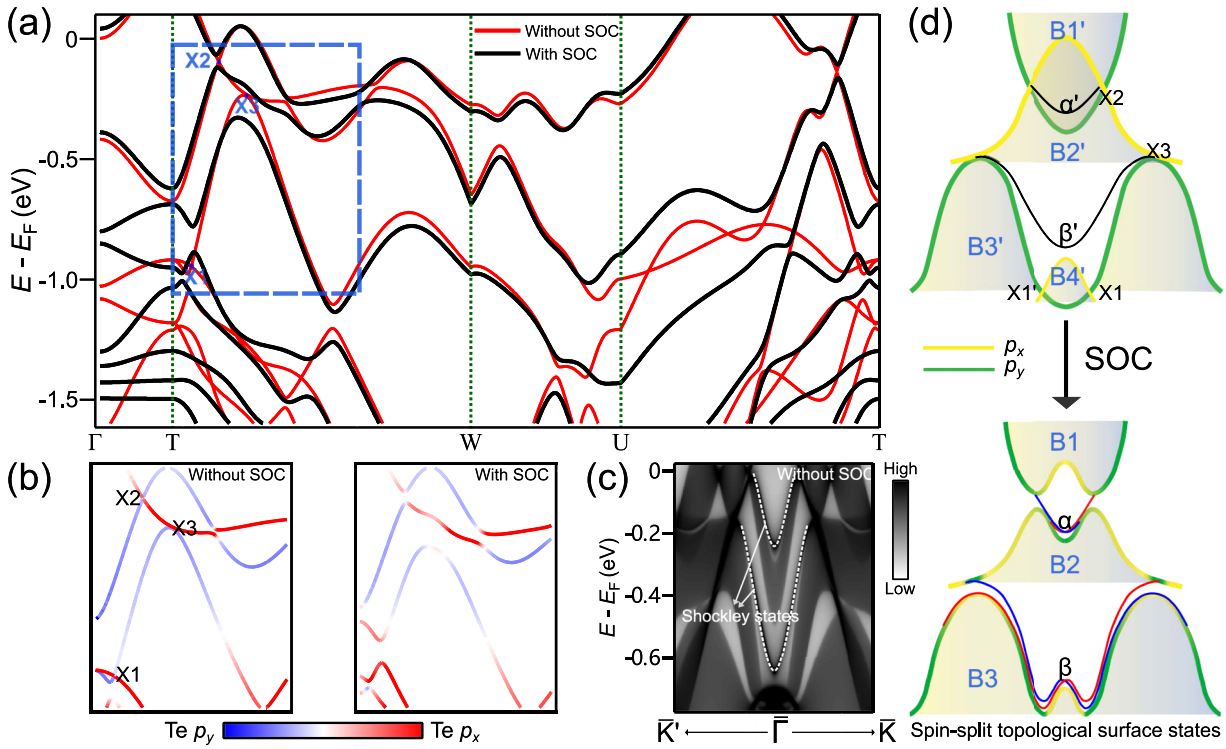

FIG. 2. (a) Comparation between calculated bulk band structures along several high-symmetry directions without (red curves) and with (black curves) SOC. (b) Contributions from p_x (red) and p_y (blue) orbits of Te $5p$ without (left) and with (right) SOC in the bule rectangle region of (a). (c) Shockley surface states revealed by tight-binding calculations without SOC. (d) Schematic diagrams of the evolution of α and β Shockley surface states.

which are denoted as X1, X2, and X3, respectively. The deeper mechanism of band inversions can be understood from the orbital composition shown in Fig. 2(b) which zooms in on the blue rectangle region in Fig. 2(a). The band inversion of Te p_x and p_y orbitals can be clearly observed even in the absence of SOC, which indicates their crystal-field-induced essence. As has been mentioned above, Shockley surface states may arise in the gaps of inverted bulk bands induced by crystal field.

The evolution of these Shockley surface bands denoted as α and β with (or α' and β' without) SOC is shown in Fig. 2(d). The Shockley surface states that connect the crossing points exist even in the absence of SOC, as indicated by the tight-binding calculations in Fig. 2(c). Because of their topologically nontrivial essence due to the band inversions, after considering SOC, the crossing points of bulk bands are gapped and each surface band splits into two branches that connect the adjacent bulk bands.

To further confirm the topological properties, the four Z_2 topological invariants ($\nu 0$, $\nu 1$, $\nu 2$, and $\nu 3$) were calculated by the Wannier charge center method [27–29] on six time-reversal invariant planes (k_x, k_y, and $k_z = 0, \pi$) using the WANNIERTOOLS package. The bulk bands B1, B2, and B3 are fully gapped throughout the BZ; thus the estimations of Z_2 topological invariants could be performed. The results are shown in Supplemental Fig. S2 (S3) [30], which indicate that the Z_2 topological invariants between B1 (B2) and B2 (B3) are (1, 000) and suggest the nontrivial topological character of the surface bands in these gaps.

It is worth discussing the origin and evolution of β bands. According to the DFT calculations, the β (β') bands are mainly derived from p_y orbitals so that their band structures basically follow the bulk p_y bands. The β' bands connecting both X3 points show a simple parabolic shape without hybridization between p_x and p_y bands in the absence of SOC. If there is no band inversion of the B3′ and B4′ bands, the β bands should exhibit a Rashba-type structure like the α bands after considering SOC. However, while the inversion exists, another upward bending occurs around the $\bar{\Gamma}$ point because the β band tends to keep the shape of the B3 band which is the hybridization of the B3′ and B4′ bands with major B4′ contribution around the $\bar{\Gamma}$ point, as illustrated in the bottom schematic diagram of Fig. 2(d). The two branches of β bands connect the gapped B2 and B3 bands and intersect only at $\bar{\Gamma}$ point.

The existence of α and β surface bands was confirmed by HRARPES measurements. As shown in Figs. 3(a) and 3(b), two parabolic α surface bands are clearly observed which are absent in the calculations of bulk bands shown in Fig. 3(c). The observed parabolalike α bands have the Rashba-type feature which is consistent with the theoretical prediction shown in Fig. 3(d). As for β bands, the ω-shaped bending structure that has been mentioned could also be seen from the second derivative image in Fig. 3(b) and the calculation results shown

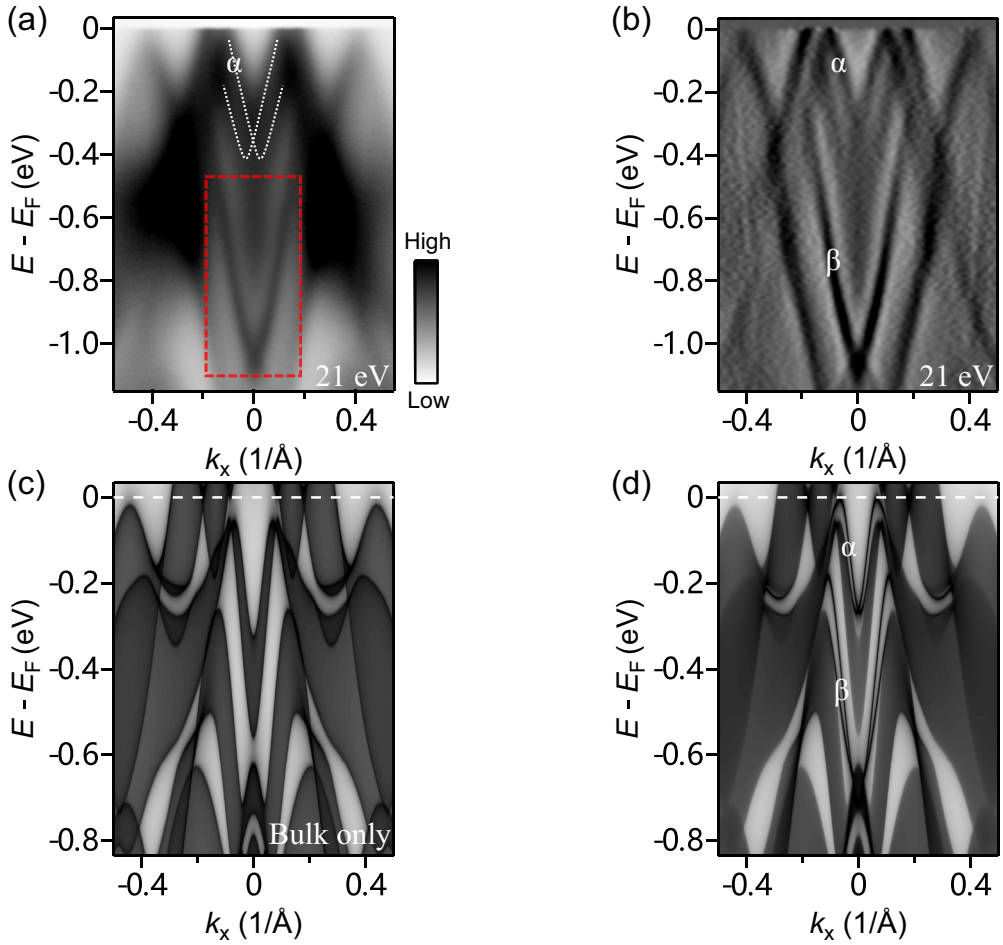

FIG. 3. (a) Experimental band structure along the $\bar{\Gamma}$-$\bar{K}$ direction measured with 21 eV photon energy by HRARPES with the Rashba-type structure of α indicated by white dashed curves. (b) Second derivative image of (a). Tight-binding calculated (c) bulk only and (d) surface and bulk band structures.

in Figs. 3(d) and 4(a). However, the two branches of β bands shown in Figs. 3(d) and 4(a) could not be well distinguished by HRARPES measurements for their tiny splitting and the existence of band broadening.

Fortunately, after the upgrade of our homemade image-type SARPES spectrometer, its energy resolution has been improved from 37 to 12 meV, which makes it possible to resolve the two branches of β bands by spin resolvability. Now we focus on the spin structure of β bands. Figure 4(b) shows the observed SARPES image in the red dashed rectangle of Fig. 3(a). The measured spin direction is in plane and perpendicular to momentum. The spin-polarized structure can be observed obviously, and the spin reverse occurs around the $\bar{\Gamma}$ point, which proves that the band splitting of β bands does exist. The calculated spin-polarized electronic states of β bands are present in Fig. 4(d), where the red (blue) color represents up-spin (down-spin) electronic states and the black (white) color represents high (low) intensity. The good agreement between experimental and theoretical results on the spin structures confirms that the two spin-polarized branches consist of β bands. Meanwhile, the ω-shaped bending structure of β bands could also be seen clearly from $k_x = \pm 0.08$ Å^{-1} to the $\bar{\Gamma}$ point, which is consistent with the above discussion.

The experimental spin structure of the α bands is shown in Fig. 4(c). It is clear to see that the α bands show significant spin polarization, which is consistent with the calculated spin structure in Fig. 4(e). Compared with the calculated results, the α bands show a very broad structure which may due to their coupling with adjacent bulk states. Under this consideration, the α states near the B2 band are probably surface resonance states and their spin polarization vanished with the influence of spin-degenerated bulk states.

IV. CONCLUSIONS

In summary, we revealed two pairs of topological Shockley surface bands in ternary compound $SnSb_2Te_4$ by using first-principles and tight-binding calculations. One shows the Rashba-type structure and the other shows a ω-shaped bending structure. The existence of the topological Shockley surface bands was confirmed by HRARPES and SARPES measurements. Our work has made it clear that the appearance of these topological Shockley surface bands is caused by the crystal-field-induced band inversions of Te p_x and p_y orbitals,

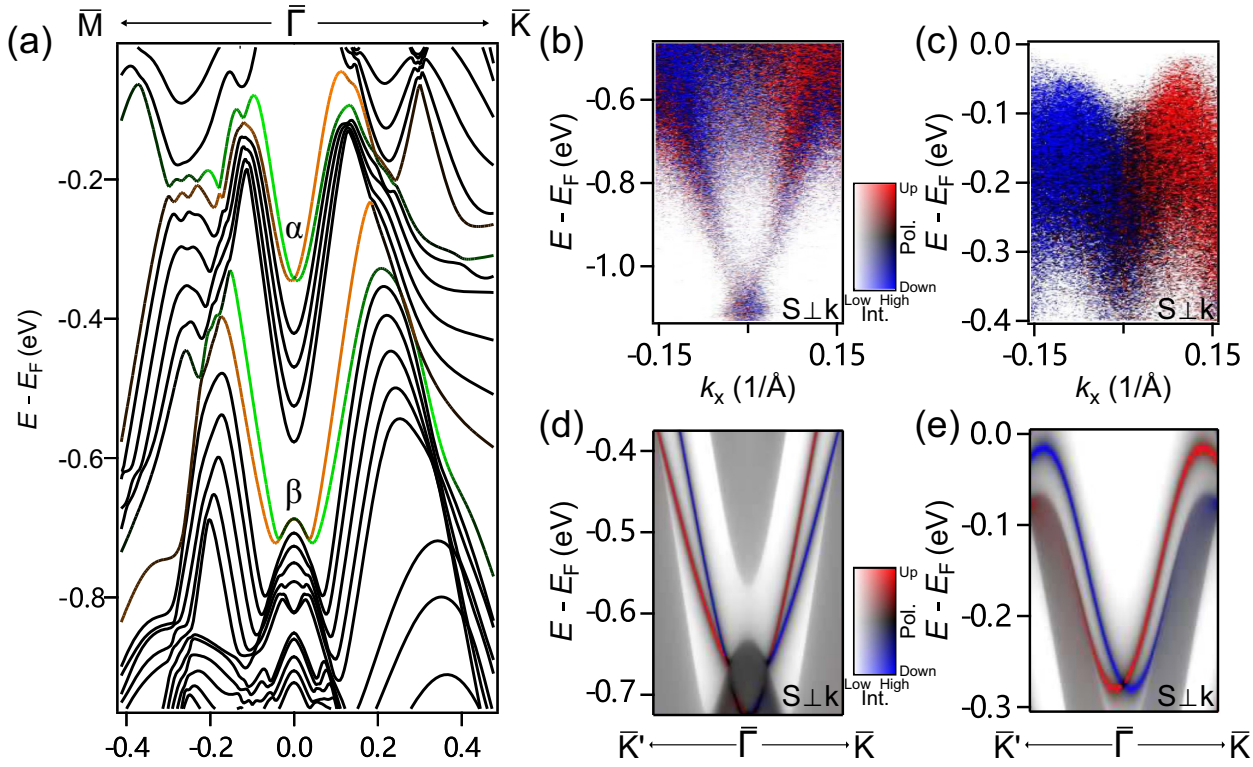

FIG. 4. (a) Band structure along $\bar{M}$-$\bar{\Gamma}$-$\bar{K}$ from slab calculations with SOC, in which the surface components are denoted by orange and green curves, and the bulk components are denoted by black curves. (b) and (c) SARPES spectra of β and α bands along the $\bar{\Gamma}$-$\bar{K}$ direction with the spin direction in plane and perpendicular to momentum. (d) and (e) Calculated spin structures corresponding to the spectra shown in (b) and (c), respectively.

and the band structure is strongly affected by the SOC-related hybridization between the two orbitals. The observation of topological Shockley surface states in $SnSb_2Te_4$ sheds new light on the extensively researched Bi_2Se_3 family, which provides a new platform to study novel topological properties in materials.

ACKNOWLEDGMENTS

This work is supported by National Natural Science Foundation of China Grants No. U1632266, No. U2032207, and No. 11927807. M.Y. acknowledges the support from National Key R&D Program of China Grant No. 2017YFA0305400.

[1] L. Fu, C. L. Kane, and E. J. Mele, Phys. Rev. Lett. **98**, 106803 (2007).
[2] Y. L. Chen, J. G. Analytis, J.-H. Chu, Z. K. Liu, S.-K. Mo, X. L. Qi, H. J. Zhang, D. H. Lu, X. Dai, Z. Fang, S. C. Zhang, I. R. Fisher, Z. Hussain, and Z.-X. Shen, Science **325**, 178 (2009).
[3] D. Hsieh, Y. Xia, D. Qian, L. Wray, F. Meier, J. H. Dil, J. Osterwalder, L. Patthey, A. V. Fedorov, H. Lin, A. Bansil, D. Grauer, Y. S. Hor, R. J. Cava, and M. Z. Hasan, Phys. Rev. Lett. **103**, 146401 (2009).
[4] Z. K. Liu, L. X. Yang, S.-C. Wu, C. Shekhar, J. Jiang, H. F. Yang, Y. Zhang, S.-K. Mo, Z. Hussain, B. Yan, C. Felser, and Y. L. Chen, Nat. Commun. **7**, 12924 (2016).
[5] J. N. Hancock, J. L. M. van Mechelen, A. B. Kuzmenko, D. van der Marel, C. Brune, E. G. Novik, G. V. Astakhov, H. Buhmann, and L. W. Molenkamp, Phys. Rev. Lett. **107**, 136803 (2011).
[6] V. M. Pereira, C. N. Wu, L. H. Tjeng, and S. G. Altendorf, Phys. Rev. Materi. **5**, 034201 (2021).
[7] M. Nurmamat, K. Okamoto, S. Y. Zhu, T. V. Menshchikova, I. P. Rusinov, V. O. Korostelev, K. Miyamoto, T. Okuda, T. Miyashita, X. X. Wang *et al.*, ACS Nano **14**, 9059 (2020).
[8] T. V. Menshchikova, S. V. Eremeev, Yu. M. Koroteev, V. M. Kuznetsov, and E. Chulkov, JETP Lett. **93**, 15 (2011).
[9] S. V. Eremeev, G. Landolt, T. V. Menshchikova, B. Slomski, Y. M. Koroteev, Z. S. Aliev, M. B. Babanly, J. Henk, A. Ernst, L. Patthey *et al.*, Nat. Commun. **3**, 635 (2012).
[10] S. Souma, K. Eto, M. Nomura, K. Nakayama, T. Sato, T. Takahashi, K. Segawa, and Y. Ando, Phys. Rev. Lett. **108**, 116801 (2012).
[11] K. Kuroda, H. Miyahara, M. Ye, S. V. Eremeev, Yu. M. Koroteev, E. E. Krasovskii, E. V. Chulkov, S. Hiramoto, C. Moriyoshi, Y. Kuroiwa, K. Miyamoto, T. Okuda, M. Arita, K. Shimada, H. Namatame, M. Taniguchi, Y. Ueda, and A. Kimura, Phys. Rev. Lett. **108**, 206803 (2012).
[12] T. Okuda, T. Maegawa, M. Ye, K. Shirai, T. Warashina, K. Miyamoto, K. Kuroda, M. Arita, Z. S. Aliev, I. R. Amiraslanov,

M. B. Babanly, E. V. Chulkov, S. V. Eremeev, A. Kimura, H. Namatame, and M. Taniguchi, Phys. Rev. Lett. **111**, 206803 (2013).
[13] B. Yan, B. Stadtmüller, N. Haag, S. Jakobs, J. Seidel, D. Jungkenn, S. Mathias, M. Cinchetti, M. Aeschlimann, and C. Felser, Nat. Commun. **6**, 10167 (2015).
[14] P. Zhang, J. Z. Ma, Y. Ishida, L.-X. Zhao, Q.-N. Xu, B.-Q. Lv, K. Yaji, G.-F. Chen, H.-M. Weng, X. Dai, Z. Fang, X.-Q. Chen, L. Fu, T. Qian, H. Ding, and S. Shin, Phys. Rev. Lett. **118**, 046802 (2017).
[15] C. Seibel, H. Bentmann, J. Braun, J. Minar, H. Maass, K. Sakamoto, M. Arita, K. Shimada, H. Ebert, and F. Reinert, Phys. Rev. Lett. **114**, 066802 (2015).
[16] C. Seibel, H. Maaß, H. Bentmann, J. Braun, K. Sakamoto, M. Arita, K. Shimada, J. Minar, H. Ebert, and F. Reinert, J. Electron Spectrosc. Relat. Phenom. **201**, 110 (2015).
[17] T. V. Menshchikova, S. V. Eremeev, and E. V. Chulkov, Appl. Surf. Sci. **267**, 1 (2013).
[18] G. Kresse and J. Hafner, Phys. Rev. B **47**, 558 (1993).
[19] G. Kresse and J. Furthmuller, Phys. Rev. B **54**, 11169 (1996).
[20] G. Kresse and D. Joubert, Phys. Rev. B **59**, 1758 (1999).
[21] N. Marzari and D. Vanderbilt, Phys. Rev. B **56**, 12847 (1997).
[22] A. A. Mostofi, J. R. Yates, Y. S. Lee, I. Souza, D. Vanderbilt, and N. Marzari, Comput. Phys. Commun. **178**, 685 (2008).
[23] Q. S. Wu, S. Zhang, H. F. Song, M. Troyer, and A. A. Soluyanov, Comput. Phys. Commun. **224**, 405 (2018).
[24] Y. C. Yang, Z. T. Liu, J. S. Liu, Z. H. Liu, W. L. Liu, X. L. Lu, H. P. Mei, A. Li, M. Ye, S. Qiao, and D. W. Shen, Nucl. Sci. Technol. **32**, 31 (2021).
[25] Z. P. Sun, Z. H. Liu, Z. T. Liu, W. L. Liu, F. Y. Zhang, D. W. Shen, M. Ye, and S. Qiao, J. Synchrotron Radiat. **27**, 1388 (2020).
[26] F. H. Ji, T. Shi, M. Ye, W. S. Wan, Z. Liu, J. J. Wang, T. Xu, and S. Qiao, Phys. Rev. Lett. **116**, 177601 (2016).
[27] L. Fu and C. L. Kane, Phys. Rev. B **76**, 045302 (2007).
[28] A. A. Soluyanov and D. Vanderbilt, Phys. Rev. B **83**, 235401 (2011).
[29] H. M. Weng, X. Dai, and Z. Fang, MRS Bull. **39**, 849 (2014).
[30] See Supplemental Material at http://link.aps.org/supplemental/10.1103/PhysRevB.106.045119 for theoretical methods and the results of Z_2 topological invariants calculations, which were used to confirm the topological properties of $SnSb_2Te_4$.